Catalysis Science & Technology

COMMUNICATION

View Article Online
View Journal

Cite this: DOI: 10.1039/c5cy00038f

Received 9th January 2015,
Accepted 27th February 2015

DOI: 10.1039/c5cy00038f

www.rsc.org/catalysis

Conjugated microporous polymers with chiral BINAP ligand built-in as efficient catalysts for asymmetric hydrogenation†

Xu Wang, Sheng-mei Lu, Jun Li, Yan Liu* and Can Li*

A series of chiral conjugated microporous polymers (CMPs) based on the chiral (*R*)-BINAP ligand (BINAP-CMPs) were synthesized with tunable BET surface areas. These solid catalysts show high activities and enantioselectivities for the asymmetric hydrogenation of β-keto esters after coordination with ruthenium species. Moreover, CMPs can realize spatial isolation. Through preventing the formation of dimers and trimers, BINAP-CMPs show much higher activity than BINAP for the Ir-catalyzed asymmetric hydrogenation of quinaldine.

Asymmetric catalysis has been developed as a powerful strategy to obtain organic molecules in their optically active forms. Compared to the significant developments in homogeneous asymmetric catalysis, heterogeneous asymmetric catalysis has received less attention and has developed slowly, in spite of its potential practicality. Actually, in most of the heterogeneous asymmetric systems, the catalytic units are normally distributed in the pore structures of the supports,[1,2] which may cause pore blocking, thus leading to a decrease in the selectivities and activities.[3] Recently, the emergence of porous organic materials, including porous organic polymers (POPs),[4–6] metal–organic frameworks (MOFs),[7] and covalent organic frameworks (COFs),[8] offers opportunities for developing new strategies in heterogeneous asymmetric catalysis.

Conjugated microporous polymers (CMPs) are new kinds of POPs, which have captured great interest. Apart from the advantages of common POPs, such as large surface areas and high stability, the porous structure and surface area of CMPs can be finely controlled at molecular level through the rigid node–strut topology of the monomer structure.[9–11] Moreover, the functional groups embedded on CMPs can be fully exposed, unlike the common mesoporous organosilicas (PMOs), which always have some of the functional groups buried in the pore wall.[12] On the other hand, compared with crystalline COFs and MOFs, amorphous CMPs can be synthesized more easily by linking the appropriate organic building units to achieve functionalization. Since the pioneering work on CMPs in 2007 by Cooper,[10] various chemical reactions, building blocks and synthetic methods have been developed for synthesizing CMPs with different structures and specific properties. Consequently, CMPs have shown many potential applications in the fields of gas storage, molecular separation, light harvesting, supercapacitive energy storage, *etc.*[13] Moreover, CMPs functionalized with catalytic units can be regarded as heterogeneous catalysts. For example, Jiang and co-workers reported the synthesis of CMP-type iron porphyrin (FeP–CMP) networks *via* a Suzuki–Miyaura coupling reaction.[14] The FeP–CMP showed high activity and selectivity as a heterogeneous catalyst for the oxidation of sulfides to sulfoxide under ambient conditions. Cooper's group developed bpy-ligated metal–organic CMPs, which can be regarded as efficient heterogeneous catalysts for reductive amination.[15] The same group also integrated Rose Bengal dye into the skeleton of CMPs. The resulting polymers showed high activity for heterogeneous photocatalytic aza-Henry reactions for a wide range of substrates.[16] Deng's group synthesized a class of metal-functionalized CMPs with salen–Co/Al complexes and 1,3,5-triethynylbenzene, which showed excellent activity for the conversion of propylene oxide to propylene carbonate under mild experimental conditions.[17] For other catalytic CMPs, see ref. 18. Despite these important advances, however, to the best of our knowledge, applying chiral CMPs as heterogeneous catalysts has not been reported. We envisioned that chiral organometallic catalysts could be introduced into the structure of CMPs. Not only do these chiral CMPs act as heterogeneous catalysts with fine-tunable structures, but also the connatural topological structure can prevent the formation of dimers and trimers, which are regarded as deactivated species in some cases (Scheme 1).

State Key Laboratory of Catalysis, Dalian Institute of Chemical Physics, Chinese Academy of Sciences, Dalian 116023, China. E-mail: yanliu503@dicp.ac.cn, canli@dicp.ac.cn

† Electronic supplementary information (ESI) available: General remarks, experimental procedure, physical and spectroscopic data for new compounds, and NMR spectra. See DOI: 10.1039/c5cy00038f

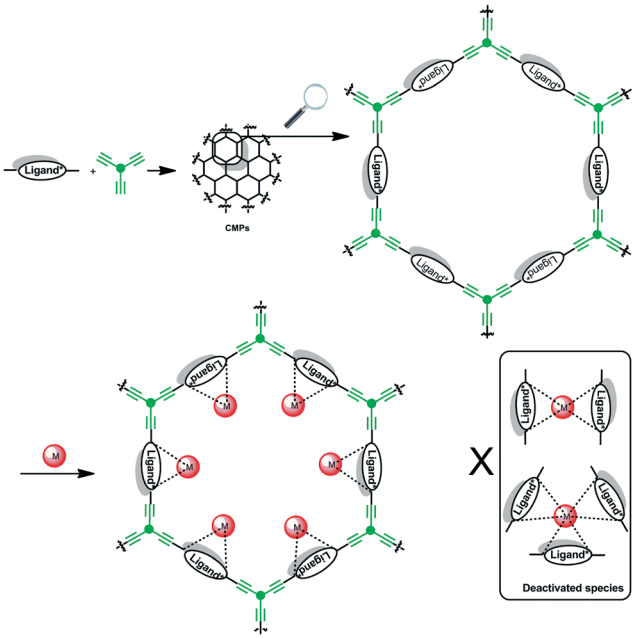

Scheme 1 The design of chiral CMPs.

Herein, we report the synthesis of four robust chiral CMPs based on the chiral (*R*)-BINAP ligand (BINAP-CMPs). These solids could be utilized as recyclable heterogeneous chiral catalysts, after being post-modified with Ru ions, for the asymmetric hydrogenation of β-ketoesters with up to 99% ee. Moreover, we also demonstrate that CMPs can realize spatial isolation, thus preventing the formation of dimers and trimers. As a result, the BINAP-CMPs show higher activity than BINAP for the Ir-catalyzed asymmetric hydrogenation of quinaldine.

2,2′-Bis(diphenylphosphino)-1,1′-binaphthalene (BINAP) with axial chirality was chosen as the catalytic unit for the synthesis of the CMPs because its backbone can be modified by functional groups to connect each other by linkers. Moreover, its linear molecular structure will reduce the possibility of any potential space-efficient packing, which will benefit the construction of polymer porosity. Inspired by Cooper's pioneering work where the micropore size and surface area of CMPs can be tuned by varying the strut length of the linker,[9–11] linkers (alkynes) with different lengths were used (**2**, **3**, **4**, and **5**). Thus, we could synthesize a series of chiral CMPs with tunable BET surface areas and pore size distributions, and investigate the influence of the material properties (such as the BET surface area and pore size distribution) on the activity and selectivity.

The preparation of the BINAPO-CMPs was carried out by a Sonogashira–Hagihara reaction of (*R*)-4,4′-dibromo BINAPO (**1**) with alkynes of different lengths (Scheme 2). Such polycondensation reactions led to four inherent porous polymers with built-in chiral BINAP platforms. We examined the cross-coupling polycondensation reactions under different conditions, including base, solvents, temperature, *etc.*, with the aim of achieving maximum surface areas for the resulting

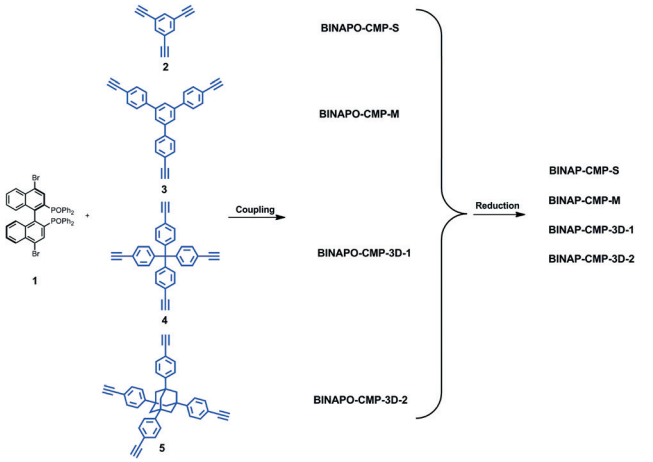

Scheme 2 Synthetic route for the BINAP-CMPs.

materials. Different optimal conditions were found for the different substituted alkynes coupling with (*R*)-4,4′-dibromo BINAPO. After repeated rinsing with chloroform, water, methanol and acetone, the CMPs were rigorously washed by Soxhlet extraction with methanol to remove any unreacted monomer or catalyst residues, and then dried at 50 °C for 24 hours under vacuum. These CMPs are insoluble in water and common organic solvents due to their cross-linked networks. TGA results showed that the decomposition of these framework starts at 300 °C (Fig. S5, ESI†).

The surface properties of the BINAPO-CMPs were investigated by nitrogen adsorption/desorption experiments at 77 K (Fig. 1A). The Brunauer–Emmett–Teller surface areas ranged from 391 $m^2\ g^{-1}$ to 509 $m^2\ g^{-1}$ (Table 1). By comparing **BINAPO-CMP-S** (monomer **2**) and **BINAPO-CMP-M** (monomer **3**), we found that the CMP with a longer strut length had a higher BET surface area (391 $m^2\ g^{-1}$ *vs.* 407 $m^2\ g^{-1}$). Similar results were found for **BINAPO-CMP-3D-1** (monomer **4**) and **BINAPO-CMP-3D-2** (monomer **5**) (474 $m^2\ g^{-1}$ *vs.* 509 $m^2\ g^{-1}$). Correspondingly, the pore sizes were mainly distributed around 1–2 nm for **BINAPO-CMP-S** and **BINAPO-CMP-M**. For **BINAPO-CMP-3D-1** and **BINAPO-CMP-3D-2**, a distribution at about 0.6 nm was found as well as a distribution around 1–2 nm (Fig. 1B).

All polymers in the series were characterized at the molecular level by ^1H–^{13}C CP/MAS NMR spectroscopy. As shown in

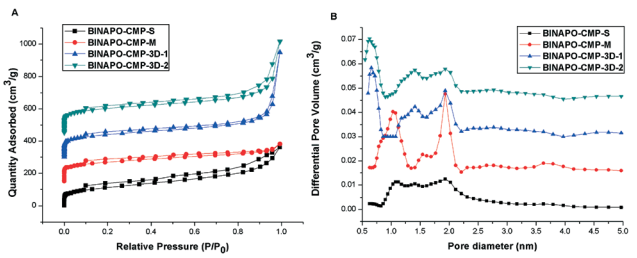

Fig. 1 (A) Nitrogen adsorption isotherms measured at 77 K for the BINAPO-CMPs. (B) Pore size distribution (PSD) for the BINAPO-CMPs, calculated by non-local density functional theory (NLDFT).

Table 1 Physical properties of the BINAPO-CMPs

Polymer	S_{BET}[a] ($m^2\ g^{-1}$)	S_{micro}[b] ($m^2\ g^{-1}$)	V_{total}[c] ($cm^3\ g^{-1}$)	V_{micro}[b] ($cm^3\ g^{-1}$)
BINAPO-CMP-S	391	146	0.56	0.07
BINAPO-CMP-M	407	261	0.36	0.13
BINAPO-CMP-3D-1	474	298	1.00	0.15
BINAPO-CMP-3D-2	509	334	0.88	0.17

[a] Surface area calculated from the N_2 adsorption isotherm using the Brunauer–Emmett–Teller method. [b] Micropore surface area and micropore volume calculated using the *t*-plot method based on the Halsey thickness equation. [c] Total pore volume at $P/P_0 = 0.99$.

Fig. 2A, the region ranging from about 110 ppm to 150 ppm corresponds to the aromatic groups in the networks. The peaks emerging at about 90 ppm represent the alkynyl groups in the polymers. The results prove the successful synthesis of the chiral CMP networks. The FT-IR spectra, in which the multi-substituted aromatic alkyne shows sharp peaks at around 3300 cm^{-1} which are weakened in the networks, also confirm the high copolymerization of dibromo BINAPO with multi-substituted aromatic alkynes in the synthesized polymers (Fig. 2C).

Next, we needed to reduce the BINAPO group embedded in the CMPs into BINAP for the asymmetric catalysis application. The BINAPO-CMPs were deoxygenated using the reported procedure[12] and the whole process was monitored by ^{31}P MAS NMR spectroscopy (Fig. 2B). In the ^{31}P MAS NMR spectrum, the BINAPO-CMP shows a broad peak centered at about 25.1 ppm assigned to phosphorus in phosphine oxide. After the reduction, a clean signal at −15.8 ppm, which can be assigned to the reduced phosphine, shows the complete reduction of BINAPO to BINAP. This result also suggests that most of the BINAPO groups are exposed in the pore as we proposed.

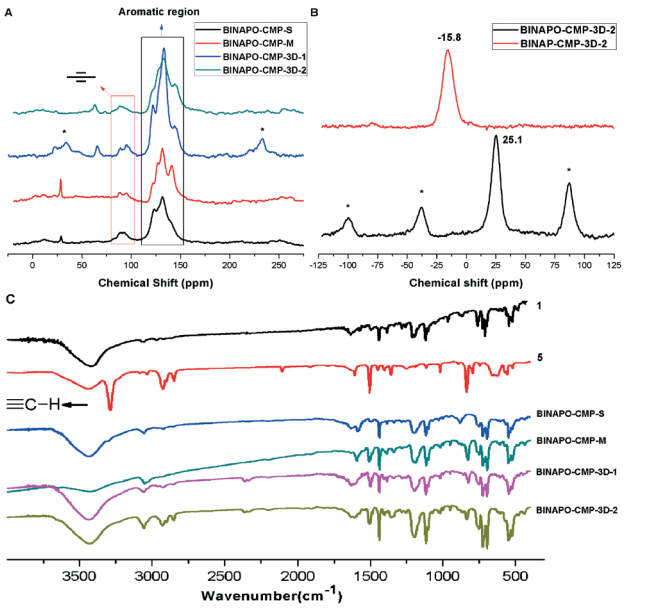

Fig. 2 (A) Solid-state ^{1}H–^{13}C CP/MAS NMR spectra for the BINAPO-CMPs, (B) solid-state ^{31}P CP/MAS NMR spectra for **BINAPO-CMP-3D-2** and **BINAP-CMP-3D-2**, (C) FT-IR spectra of (*R*)-4,4-dibromo-BINAPO **1**, 1,3,5,7-tetrakis(4-ethynylphenyl)adamantine **5** and the BINAPO-CMPs.

With the BINAP-CMPs in hand, to evaluate their catalytic activity as robust heterogeneous catalysts, we accordingly chose the asymmetric hydrogenation reaction of methyl acetoacetate as a model reaction.[19] Under the same reaction conditions, all the BINAP-CMPs combined with $[Ru(benzene)Cl_2]_2$ were tested as chiral catalysts. The results are shown in Table 2. We found that all the CMPs showed similar conversions ranging from 24% to 30% in 2 hours, but varying ee values. The **Ru/BINAP-CMPs-3D-2** catalyst achieved a much better ee value than the others. In view of the structural data of **BINAP-CMPs-3D-2** (Table S2, ESI†), the large BET surface area and micropore volume may play important roles in the better activity and enantioselectivity. It is understandable that the CMPs with larger BET surface areas and micropore volumes may benefit from the diffusion of the substrate and product, which makes it easier to access the active center and then improve the reaction performance.

Additionally, a number of different substituted β-keto esters could be completely converted into the corresponding chiral alcohols on **Ru/BINAP-CMP-3D-2** with 0.1 mol% catalyst loading (Table 3). The structures of the β-keto esters significantly affect the catalytic performance of **Ru/BINAP-CMP-3D-2**. Keto esters bearing larger substituents in the R_2 position result in a higher enantioselectivity than those bearing smaller ones. For the asymmetric hydrogenation of *tert*-butyl 3-oxobutanoate (Table 3, entry 4), the ee value could reach as high as 99%. We also found that with appropriate steric hindrance in the R_1 position, the ee value could reach as high as 92% (Table 3, entry 3). The above results suggest that **Ru/BINAP-CMP-3D-2** is an efficient catalyst for asymmetric hydrogenation. Upon completion of the reaction, the solid **Ru/BINAP-CMP-3D-2** catalyst could be readily recovered by centrifugation and a regular filter. The colorless filtrate from the asymmetric hydrogenation of methyl acetoacetate did not afford any additional product, suggesting the heterogeneous nature of the reaction system. After washing with THF and heating under vacuum, the solid catalyst was reused for the next cycle. We did not observe any significant deterioration in the activity for the recovered catalyst even after three cycles. However, the enantioselectivity decreased from 94% to 90%, (Table S1, ESI†) which may be due to the unknown changing of the microenvironment of the activity center when processing.

Table 2 Reactivity comparison experiment of the synthesized BINAP-CMPs[a]

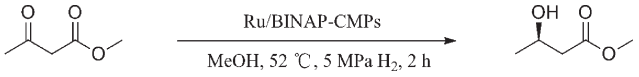

Entry	Catalyst	Conversion[b] (%)	ee[b] (%)
1	**Ru/BINAP-CMP-S**	26	67
2	**Ru/BINAP-CMP-M**	27	71
3	**Ru/BINAP-CMP-3D-1**	24	72
4	**Ru/BINAP-CMP-3D-2**	30	91

[a] Reaction conditions: 5 mmol of methyl acetoacetate in 2 mL of MeOH, 0.0025 mmol $[Ru(benzene)Cl_2]_2$, 5 MPa H_2, 52 °C for 2 h. [b] The conversion and ee values were determined by GC on a Supelco γ-DEX 225 capillary column.

Table 3 Asymmetric hydrogenation of β-keto esters catalyzed by the **Ru/BINAP-CMP-3D-2** catalyst[a]

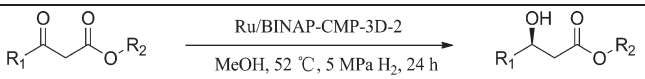

Entry	*R*	Conversion[b] (%)	ee[b] (%)
1	R_1 = Me, R_2 = Me	99	94
2	R_1 = Me, R_2 = Et	99	93
3	R_1 = $ClCH_2$, R_2 = Me	99	92
4	R_1 = Me, R_2 = ^{t}Bu	99	99
5	R_1 = Me, R_2 = CH_2-Ph	99	95
6	R_1 = Me, R_2 = ^{i}Pr	99	94
7	R_1 = Et, R_2 = Me	99	90
8[c]	R_1 = ^{i}Pr, R_2 = Me	99	90
9[d]	R_1 = Me, R_2 = Me	99	99

[a] Reaction conditions: 5 mmol of β-keto esters in 2 mL of MeOH, 0.0025 mmol $[Ru(benzene)Cl_2]_2$, 5 MPa H_2, 52 °C for 24 h. [b] The conversion and ee values were determined by GC on a Supelco γ-DEX 225 capillary column. [c] Reaction time = 48 h. [d] The use of homogeneous Ru/BINAP catalyst.

In Ir-catalyzed asymmetric hydrogenation, irreversible formation of inactive dimers and trimers through hydride-bridged bonds is regarded as the deactivation factor, which results in high catalyst loadings.[20] For example, in the asymmetric hydrogenation of quinaldine, Ir-BINAPs are always used as catalysts with high loadings.[21] Encouraged by the natural structure of BINAP-CMPs, which should inhibit the formation of dimers and trimers, we applied the BINAP-CMPs to the Ir-catalyzed asymmetric hydrogenation of quinaldine. In the preliminary investigations for this reaction, the BINAP-CMPs combined with Ir showed much higher activity than the homogeneous BINAP/Ir catalytic system (Table 4).

Conclusions

In summary, we have synthesized a series of BINAP-CMPs with tunable BET surface areas, which show high activities and enantioselectivities for the asymmetric hydrogenation of β-keto esters after coordination with ruthenium species. Moreover, we found that the catalytic performance of the CMPs was related to the structure properties of the CMPs. The BINAP-CMPs were also used for the iridium-catalysed asymmetric reactions of quinaldine and they show much higher activity than BINAP because they prevent the formation of dimers and trimers.

Table 4 Asymmetric hydrogenation of quinaldine by the **Ir/BINAP-CMP-3D-2** catalyst[a]

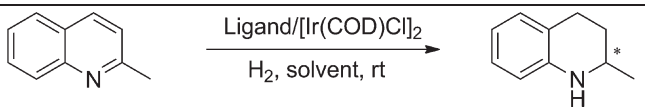

Entry	Ligand	Conversion[b] (%)	ee[c] (%)
1	BINAP	23	71
2	**BINAP-CMP-3D-2**	99	70

[a] Reaction conditions: 0.25 mmol of quinaldine in 3 mL of CH_2Cl_2, 0.00125 mmol $[Ir(COD)Cl]_2$, 0.0125 mmol I_2, 4 MPa H_2, 25 °C for 2 h. [b] Determined by ^{1}H NMR analysis of the crude product. [c] Determined by HPLC analysis with a Chiralpak OJ-H column.

Acknowledgements

We acknowledge the financial support from the National Nature Science Foundation of China (NSFC grant no. 21322202).

Notes and references

1 (*a*) D. P. Allen, M. M. Van Wingerden and R. H. Grubbs, *Org. Lett.*, 2009, **11**, 1261–1264; (*b*) H. L. Qiu, S. M. Sarkar, D. H. Lee and M. J. Jin, *Green Chem.*, 2008, **10**, 37–40; (*c*) K. V. S. Ranganath, J. Kloesges, A. H. Schafer and F. Glorius, *Angew. Chem., Int. Ed.*, 2010, **49**, 7786–7789; (*d*) S. Wittmann, A. Schatz, R. N. Grass, W. J. Stark and O. Reiser, *Angew. Chem., Int. Ed.*, 2010, **49**, 1867–1870.

2 (*a*) H. Q. Yang, G. A. Li, Z. C. Ma, J. B. Chao and Z. Q. Guo, *J. Catal.*, 2010, **276**, 123–133; (*b*) H. Q. Yang, Y. W. Wang, Y. Qin, Y. Z. Chong, Q. Z. Yang, G. Li, L. Zhang and W. Li, *Green Chem.*, 2011, **13**, 1352–1361; (*c*) H. Zhou, Y. M. Wang, W. Z. Zhang, J. P. Qu and X. B. Lu, *Green Chem.*, 2011, **13**, 644–650; (*d*) F. X. Zhu, W. Wang and H. X. Li, *J. Am. Chem. Soc.*, 2011, **133**, 11632–11640.

3 M. Gruttadauria, F. Giacalone and R. Noto, *Chem. Soc. Rev.*, 2008, **37**, 1666–1688.

4 (*a*) T. Ben, H. Ren, S. Q. Ma, D. P. Cao, J. H. Lan, X. F. Jing, W. C. Wang, J. Xu, F. Deng, J. M. Simmons, S. L. Qiu and G. S. Zhu, *Angew. Chem., Int. Ed.*, 2009, **48**, 9457–9460; (*b*) L. Chen, Y. Honsho, S. Seki and D. L. Jiang, *J. Am. Chem. Soc.*, 2010, **132**, 6742–6748; (*c*) A. I. Cooper, *Adv. Mater.*, 2009, **21**, 1291–1295; (*d*) P. Kaur, J. T. Hupp and S. T. Nguyen, *ACS Catal.*, 2011, **1**, 819–835; (*e*) N. B. McKeown and P. M. Budd, *Chem. Soc. Rev.*, 2006, **35**, 675–683.

5 (*a*) Q. Sun, X. J. Meng, X. Liu, X. M. Zhang, Y. Yang, Q. H. Yang and F. S. Xiao, *Chem. Commun.*, 2012, **48**, 10505–10507; (*b*) H. C. Cho, H. S. Lee, J. Chun, S. M. Lee, H. J. Kim and S. U. Son, *Chem. Commun.*, 2011, **47**, 917–919; (*c*) A. Trewin and A. I. Cooper, *Angew. Chem., Int. Ed.*, 2010, **49**, 1533–1535; (*d*) C. A. Wang, Z. K. Zhang, T. Yue, Y. L. Sun, L. Wang, W. D. Wang, Y. Zhang, C. Liu and W. Wang, *Chem. – Eur. J.*, 2012, **18**, 6718–6723.

6 (*a*) W. L. Wang, A. M. Zheng, P. Q. Zhao, C. Xia and F. W. Li, *ACS Catal.*, 2014, **4**, 321–327; (*b*) Z. L. Li, J. H. Liu, C. G. Xia and F. W. Li, *ACS Catal.*, 2013, **3**, 2440–2448; (*c*) Z. Wang, G. Chen and K. L. Ding, *Chem. Rev.*, 2009, **109**, 322–359; (*d*) L. Shi, X. W. Wang, C. A. Sandoval, Z. Wang, H. J. Li, J. Wu, L. T. Yu and K. L. Ding, *Chem. – Eur. J.*, 2009, **15**, 9855–9867; (*e*) X. W. Wang, L. Shi, M. X. Li and K. L. Ding, *Angew. Chem., Int. Ed.*, 2005, **44**, 6362–6366.

7 (*a*) F. J. Song, C. Wang, J. M. Falkowski, L. Q. Ma and W. B. Lin, *J. Am. Chem. Soc.*, 2010, **132**, 15390–15398; (*b*) C. D. Wu, A. Hu, L. Zhang and W. B. Lin, *J. Am. Chem. Soc.*, 2005, **127**, 8940–8941.

8 (*a*) S. Y. Ding, J. Gao, Q. Wang, Y. Zhang, W. G. Song, C. Y. Su and W. Wang, *J. Am. Chem. Soc.*, 2011, **133**, 19816–19822; (*b*) S. Y. Ding and W. Wang, *Chem. Soc. Rev.*, 2013, **42**, 548–568; (*c*) X. Feng, X. S. Ding and D. L. Jiang, *Chem. Soc. Rev.*, 2012, **41**, 6010–6022.

9 R. Dawson, A. Laybourn, Y. Z. Khimyak, D. J. Adams and A. I. Cooper, *Macromolecules*, 2010, **43**, 8524–8530.

10 J. X. Jiang, F. Su, A. Trewin, C. D. Wood, N. L. Campbell, H. Niu, C. Dickinson, A. Y. Ganin, M. J. Rosseinsky, Y. Z. Khimyak and A. I. Cooper, *Angew. Chem., Int. Ed.*, 2007, **46**, 8574–8578.

11 J. X. Jiang, F. Su, A. Trewin, C. D. Wood, H. Niu, J. T. A. Jones, Y. Z. Khimyak and A. I. Cooper, *J. Am. Chem. Soc.*, 2008, **130**, 7710–7720.

12 P. Y. Wang, X. Liu, J. Yang, Y. Yang, L. Zhang, Q. H. Yang and C. Li, *J. Mater. Chem.*, 2009, **19**, 8009–8014.

13 (*a*) Y. Kou, Y. H. Xu, Z. Q. Guo and D. L. Jiang, *Angew. Chem., Int. Ed.*, 2011, **50**, 8753–8757; (*b*) A. Li, H. X. Sun, D. Z. Tan, W. J. Fan, S. H. Wen, X. J. Qing, G. X. Li, S. Y. Li and W. Q. Deng, *Energy Environ. Sci.*, 2011, **4**, 2062–2065; (*c*) W. G. Lu, D. Q. Yuan, D. Zhao, C. I. Schilling, O. Plietzsch, T. Muller, S. Brase, J. Guenther, J. Blumel, R. Krishna, Z. Li and H. C. Zhou, *Chem. Mater.*, 2010, **22**, 5964–5972; (*d*) Y. H. Xu, A. Nagai and D. L. Jiang, *Chem. Commun.*, 2013, **49**, 1591–1593.

14 L. Chen, Y. Yang and D. L. Jiang, *J. Am. Chem. Soc.*, 2010, **132**, 9138–9143.

15 J. X. Jiang, C. Wang, A. Laybourn, T. Hasell, R. Clowes, Y. Z. Khimyak, J. L. Xiao, S. J. Higgins, D. J. Adams and A. I. Cooper, *Angew. Chem., Int. Ed.*, 2011, **50**, 1072–1075.

16 J. X. Jiang, Y. Y. Li, X. F. Wu, J. L. Xiao, D. J. Adams and A. I. Cooper, *Macromolecules*, 2013, **46**, 8779–8783.

17 (*a*) Y. Xie, T. T. Wang, X. H. Liu, K. Zou and W. Q. Deng, *Nat. Commun.*, 2013, **4**, 1960; (*b*) Y. Xie, R. X. Yang, N. Y. Huang, H. J. Luo and W. Q. Deng, *J. Energy Chem.*, 2014, **23**, 22–28.

18 (*a*) Z. G. Xie, C. Wang, K. E. deKrafft and W. B. Lin, *J. Am. Chem. Soc.*, 2011, **133**, 2056–2059; (*b*) N. Kang, J. H. Park, K. C. Ko, J. Chun, E. Kim, H. W. Shin, S. M. Lee, H. J. Kim, T. K. Ahn, J. Y. Lee and S. U. Son, *Angew. Chem., Int. Ed.*, 2013, **52**, 6228–6232.

19 (*a*) M. Berthod, C. Saluzzo, G. Mignani and M. Lemaire, *Tetrahedron: Asymmetry*, 2004, **15**, 639–645; (*b*) A. G. Hu, H. L. Ngo and W. B. Lin, *Angew. Chem., Int. Ed.*, 2004, **43**, 2501–2504; (*c*) Y. Y. Huang, Y. M. He, H. F. Zhou, L. Wu, B. L. Li and Q. H. Fan, *J. Org. Chem.*, 2006, **71**, 2874–2877; (*d*) X. Jin, F. F. Kong, Z. Q. Yang and F. F. Cui, *J. Mol. Catal. A: Chem.*, 2013, **374**, 22–26.

20 Z. J. Wang, G. J. Deng, Y. Li, Y. M. He, W. J. Tang and Q. H. Fan, *Org. Lett.*, 2007, **9**, 1243–1246.

21 (*a*) W. B. Wang, S. M. Lu, P. Y. Yang, X. W. Han and Y. G. Zhou, *J. Am. Chem. Soc.*, 2003, **125**, 10536–10537; (*b*) R. N. Guo, X. F. Cai, L. Shi, Z. S. Ye, M. W. Chen and Y. G. Zhou, *Chem. Commun.*, 2013, **49**, 8537–8539.